ATTACHMENT NUMBER THREE(3)

(2)

AD-A260 388

QUIREMENTS LIST
(ems)

Form Approved
OMB No 0704 0188

mated to average 220 hours per response, including the time for reviewing instructions, sear ching led and completing and reviewing the collection of information. Send comments regarding this mation, including suggestions for reducing this burden to Department of Defense, Washington id Reports, 1215 Jefferson Davis Highway, Suite 1204, Arlington, VA 22202-4302, and to the Office of 88), Washington, DC 20503. Please DO NOT RETURN your form to either of these addresses. Send or the Contract/PR No. listed in Block E.

A. CONTRACT LINE ITEM NO.	B. EXHIBIT	C. CATEGORY:
0001AB	B	TDP ____ TM ____ OTHER TECHNICAL REPORTS

D. SYSTEM/ITEM	E. CONTRACT/PR NO.	F. CONTRACTOR
Inexpensive Capillary Discharge XRay Laser	N00014-92-C-2218	MOXTEK

1. DATA ITEM NO.	2. TITLE OF DATA ITEM	3. SUBTITLE
B001	Mid-Term Technical Report	

4. AUTHORITY (Data Acquisition Document No.)	5. CONTRACT REFERENCE	6. REQUIRING OFFICE
	CLIN 0001AB	CODE 4720

7. DD 250 REQ	9. DIST STATEMENT REQUIRED	10. FREQUENCY	12. DATE OF FIRST SUBMISSION
DD		OTIME	120DAC
8. APP CODE		**11. AS OF DATE**	**13. DATE OF SUBSEQUENT SUBMISSION**

17. PRICE GROUP

18. ESTIMATED TOTAL PRICE

16. REMARKS

THIS REPORT IS TO PROVIDE INFORMATION ON PROGRESS UP TO DATE REGARDING THE RESEARCH WORK UNDER THE CONTRACT.

14. DISTRIBUTION	b. COPIES		
a. ADDRESSEE	Draft	Final Reg	Final Repro
CODE 4720		1	
15. TOTAL →		1	

1. DATA ITEM NO.	2. TITLE OF DATA ITEM	3. SUBTITLE

4. AUTHORITY (Data Acquisition Document No.)	5. CONTRACT REFERENCE	6. REQUIRING OFFICE

7. DD 250 REQ	9. DIST STATEMENT REQUIRED	10. FREQUENCY	12. DATE OF FIRST SUBMISSION
8. APP CODE		**11. AS OF DATE**	**13. DATE OF SUBSEQUENT SUBMISSION**

17. PRICE GROUP

18. ESTIMATED TOTAL PRICE

16. REMARKS

14. DISTRIBUTION	b. COPIES		
a. ADDRESSEE	Draft	Final Reg	Final Repro
15. TOTAL →			

G. PREPARED BY	H. DATE	I. APPROVED BY	J. DATE

DD Form 1423-2, JUN 90
1059/183 S/N 0102-LF-010-5600

Previous editions are obsolete

INEXPENSIVE CAPILLARY DISCHARGE X-RAY LASER DRIVER. INTERMEDIATE TECHNICAL REPORT FOR PHASE I

A. M. PANIN 1.29.93

In this report we present the results of our search for lasing schemes using a collisional pumping mechanism of active level population suitable for a capillary discharge plasma.

We have performed atomic data calculations which give us accurate figures for energy level positions for Ne-like Ar, including highly excited levels which have not been studied experimentally and which are of significant interest for short-wavelength lasing. We also calculated radiative transition probabilities as well as branch coefficients for transitions of interest for lasing. The calculations were performed not only for Ne-like ions but also for Ni-like ions of krypton and molybdenum, as the Ni-like scheme seems to be promising for scaling to lower wavelengths. Using the results of these calculations, we are able to predict possible laser lines and to estimate their relative intensities.

The Ne-like scheme for laser operation with electron-collisional pumping was predicted in [1,2]. The validity of this scheme was confirmed by several experiments with laser-produced plasma. We mention here just a few: for Ne-like Se [3], Y [4], Ti [5], Cu [6], and Ge [7-9], showing the trend to heavy elements with decreasing laser wavelength. Experiments with Z-pinch driven Ne-like Kr lasers are under performance now [10].

The Ni-like laser scheme is similar to that for Ne-like. However, it is surprising that the first observations of 4-4 transitions in heavy Ni-like ions were done without a detailed experimental investigation of the energy structure of the ions that characterizes both schemes as stable and reliable [11,12]. The experimental observations of lasing in Ni-like Eu, Yb, and W have demonstrated the advantage of the Ni-like laser scheme compared with the Ne-like scheme [11,12]. To date, laser produced plasmas are the main source for laser gain studies for transitions in multicharged ions. It was shown that induced laser radiation at the 4-4 transitions of Ni-like ions is created with a density flow of primary laser irradiation of 10^{14}-10^{15} W/cm^2. However, for the same wavelength region, laser radiation at the 3-3 transitions of Ne-like ions needs a higher flow of more than 10^{16} W/cm^2 [11,12]. These differences in plasma parameters can be explained by the difference in excitation energy of the $2p^1$ and the $3d^{10}$ core shells under the condition of equal 3p-3s and 4d-4p transition energy in Ne-like and Ni-like ions, respectively.

Theoretical investigation of the Ne-like isoelectronic sequence spectroscopic properties was performed by a number of authors

Theoretical investigation of the Ne-like isoelectronic sequence spectroscopic properties was performed by a number of authors [13-16]. Experimentally it was investigated up to Z = 60 (for 3-2 transitions) [17]. The Ni-like isoelectronic system has been studied much less. The results of experimental investigations of Ni-like ion energy levels for Z = 30-50 are summarized in [18]. Measurements of the energy of $\Delta J=1$ resonance transitions for heavy (Z > 60) Ni-like ions were analyzed in [19]. Recently, a few works have appeared which are aimed at a detailed study of the spectroscopic properties of Ni-like ions [20,21]. A theoretical investigation of Ni-like x-ray lasers resonantly photopumped by Lyman-alpha radiation was presented in [22]. We will present the calculations of energy levels positions and lifetimes of these levels in Ne-like argon, and Ni-like krypton and molybdenum. The calculations include highly excited states arising from the excitation of 2s electrons in Ne-like ions and 3p electrons in Ni-like ions. These states may be excited in a different kind of experimental plasma source. However, experimental investigation of the energy structure of these levels is difficult because of the high spectrum density and the superposition of many lines. Thus, atomic data calculations for highly excited levels can provide new ideas for generating shorter wavelength laser lines.

METHOD OF CALCULATION

The calculations were performed by the Relativistic Perturbation Theory Method with the Model Potential of zero approximation (RPTMP). This method is reliable for calculating energy levels for various isoelectronic sequences. RPTMP is especially successful in the calculation of rate constants of processes involving multicharged ions, photons, and electrons [23]. A detailed description of our calculation model is given in [13]. Here we outline the foundations of our approach which is called the energy approach [24]. In nonrelativistic theory, the field form procedure, connected with the diagonalization of the secular matrix, is the standard method for the calculation of the energy shift E of degenerate atomic states [25,26] . Our approach is based upon the Gell-Mann and Low adiabatic formula and the perturbation expansion of the scattering matrix. We use an analogous scheme with the electrodynamic scattering matrix [24]. The perturbation expansion for the energy has only even powers. The contributions are usually presented in the form of Feynman diagrams. An important advantage of the approach is the effective inclusion of high-order perturbation theory (PT) corrections [27].

In this calculation, attention is directed to finding the most suitable description of the zeroth approximation, one-particle energies and wave functions. One-electron and one-vacancy energies are counted from the $1s^2\ 2s^2\ 2p^6$ core for Ne-like ions and from the $1s^2\ 2s^2\ 2p^6\ 3s^2\ 3p^6\ 3d^{10}$ core for Ni-like ions. By definition the

total energy of one electron (or vacancy) over the core is the sum of all one-particle diagrams of all orders of the perturbation theory. Precisely determined n one-particle energies allow the computation to take into account the major part of the correlation, relativistic, and electrodynamic effects already in the zeroth-order perturbation theory. It should be stressed that the convergence of the perturbation series and the accuracy of the final results are determined in large measure by the quality of the one-particle basis function.

The total Hamiltonian of the system is

$$H=\sum_{i=1}^{N_t} h(r_i) + \sum_{i>j}^{N_t} e^{i\omega r_{ij}} \frac{(1-\alpha_i\alpha_j)}{r_{ij}} \qquad (1)$$

where the summation extends over the total number of electrons N_t; $h(r)$ is the one-electron Dirac Hamiltonian for an electron in the nuclear Coulomb field, α_i and α_j are Pauli matrices and ω is the energy difference of the initial and final two-particle states. The one-particle wave function of the zeroth approximation is determined by the solution of the relativistic Dirac equation

$$H_0=\sum_{i=1}^{N_t} h(r_i) + \sum_{j=1}^{N_t} V_c(r_i/b) \qquad (2)$$

whose eigenvalue is the exact (empirical) energy of a vacancy E_{vac} or of an electron E_{el} with the electrodynamic correction subtracted out. We present the model potential for N-electron core in the form:

$$V_c=V_c(K)+V_c(L)+V_c(M)+V_c(N)+\ldots \qquad (3)$$

where $V_c(K), V_c(L), V_c(M)$ ... are responsible for potentials of the K, L, M shells;

$$V_c(K)=2\left[1-e^{-2rb_1}(1+rb_1)\right]/r \qquad (4)$$

$$V_c(L) = 8\,[1 - e^{-rb_2}(1 + 0.75rb_2 + 0.25r^2b_2^2 + 0.625r^3b_2^3]/r \qquad (5)$$

$$V_c(M) = 18\,[1 - e^{-rb_3}(1 + \frac{5}{6}rb_3 + \frac{1}{3}r^2b_3^2 + \frac{5}{54}r^3b_3^3]/r \qquad (6)$$

The potential parameters b_1, b_2, b_3 were determined by our previous studies of isoelectronic sequences with one particle (electron or vacancy) over different kinds of cores [33, 34]. For a 10-electron core (Ne-like ions) the model potential used was [33]

$$V_c = V_c(K) + V_c(L) \qquad (7)$$

For a 28-electron core (Ni-like ions) the model potential used was [34]

$$V_c = V_c(K) + V_c(L) + V_c(M) \qquad (8)$$

Correctly chosen values of the adjustable parameter $b(nlj/Z)$ meet the conditions:

$$f(r) \to 0,\ g(r) \to 0 \ \text{at} \ r \to \infty \qquad (9)$$

where $f(r)$ and $g(r)$ are, respectively, the large and small components of the Dirac wave functions. The perturbation operator is then

$$H_{pert} = \sum_{i>j}^{N_t} e^{iwr_{ij}} \frac{(1 - \alpha_i\alpha_j)}{r_{ij}} - \sum_{i=1}^{N_t} V_c(r_i/b) \qquad (10)$$

The excitation energy of a state J, M_J is represented in the form of a perturbation theory series, i.e.,

$$E(n_1l_1j_1, n_2l_2j_2\,[JM_J]) = E_{el}^0(n_1l_1j_1) + E_{vac}^0(n_2l_2j_2) + \Delta E^{(2)} + E(4) + \ldots \qquad (11)$$

where $E_{el}{}^0\ (n_1, l_1, j_1), E_{vac}{}^0(n_2, l_2, j_2)$ are, respectively, the exact (empirical) one-particle energies of the electron above the core and vacancy in the core. In the first PT order, it is necessary to calculate only the matrix elements of the operator for the electron-vacancy interaction, that is

$$\Delta E_2 = \langle n_1 l_1 j_1 n_2 l_2 j_2 [JM_J] | \exp(iwr_{12}) \frac{1-\alpha_1\alpha_2}{r_{12}} | n_1' l_1' j_1' n_2' l_2' j_2' [JM_J] \rangle =$$

$$= [(2j_1+1)(2j1'+1)(2j_2+1)(2j_2'+1)]^{1/2} x$$

$$x [\sum_a (-1)^{j_2+j_2'+a+J} \begin{Bmatrix} a & j_1 & j_1' \\ J & j_2' & j_2 \end{Bmatrix} Q_a(12;2'1') \frac{(-1)^{j_2'+j_2}}{2J+1} Q_J(12';1'2)] \quad (12)$$

Q_a is expressed through Slater integrals and angular multiplies. Its determination is explained in [13].

Our study of the spectroscopic properties for different kinds of atomic systems has shown that in many cases the accounting for the higher-order perturbation theory corrections are important. A method of accounting for higher-order perturbation theory corrections was proposed in [27]. Second and higher-order PT Feynman diagrams are analyzed, and a simple method of accounting for them is discussed [27]. This method is especially effective in the calculation of Ne-like and Ni-like ion energy states. In both kinds of ions there are singlet levels with J=0, or J=1 characterized with a strong state interaction (superposition of states). These states are sensitive to the way correlation effects are taken into account. Some of these states are the active laser levels, so the accuracy of the theoretical prediction for these states is important. The energies of levels $2p_{3/2}$ $3p_{3/2}$ [J=0] in Ne-like ions and $3d_{5/2}$ $4d_{5/2}$ [J=0] in Ni-like ions have errors of ≈ 4 eV if the usual theoretical approaches are used to do the calculations [28]. These approaches do not account for the higher-order PT corrections. Our method allows us to reduce the computation error for the energy levels in Ne-like ions to the value of ≈ 1 eV and those in Ni-like ions to ≈ 0.2 eV. Experimental information about the energy structure of highly excited configurations is scarce in the literature both for Ne-like and Ni-like ions. This is explained by difficulties in energy transition measurements by the usual techniques because of line blending caused by the dense spectra. As a rule the accuracy of the theoretical predictions of highly excited level positions also decreases.

The energy level positions for 3d 4f [J=1] states were obtained by measuring resonance lines in Rb X-Sn XXIII [29]. The results of our calculations for these energies for Mo XV are not in good agreement with the measurements [29] (see Table 2). We did the calculations and comparisons of energy levels for the 3d4f configuration for other Ni-like ions with z = 47-50 and obtained much better agreement between theory and experiment. Based on the set of calculations and the comparisons with experimental values for

different z for Ni-like ions we conclude that the accuracy of our calculations for highly excited levels varies in limits of 0.1-1 eV for different levels.

RESULTS OF CALCULATIONS

Numerical results of our calculations for energy levels and radiative characteristics of Ne-like argon are given in Table 1. Level order numbers, quantum numbers, and total moment J are in the first three columns. Our theoretical energy levels are given in the fourth column. These energy level positions were calculated with a method that effectively accounted for higher-order perturbation theory corrections [27]. In the next column (5th) the experimental and fitting energy levels are listed (see [18]). The comparison shows agreement in limits of a few hundred cm^{-1} for all states calculated. The sixth column gives the radiative decay probabilities into the ground state $2s^2\ 2p^6$ for every state. These numbers allow us to determine low active levels, which have the largest values for radiative decay probabilities into the ground state. The seventh column gives the life-time characteristics for each level. Except for the odd states with J=1 the life time of each state is determined by radiative decays into all low lying states. All possible 4-4 and 3-3 radiative transition probabilities--electric dipole, magnetic dipole and electric quadruple transitions--are included. Forbidden transitions are of little importance. The eighth column lists the dominating decay channel, i.e., the order number of the low lying state in which the transition probability is of the largest value. In the ninth column the branch coefficient for the dominating decay channel is given. It shows the percentage of the level population decay into the dominating channel. The tenth column gives calculated wavelength for the transition into the dominating channel (level in eighth colomn) for each state, and last column gives the experimentally measured wavelength.

In Ne-like ions there are two levels $2p_{3/2}\ 3p_{3/2}$ [J = 0] and $2p_{1/2}\ 3d_{3/2}$ [J = 1] where correlation effects are difficult to take into account. The accuracy of these two calculations is ≈ 1 eV along the isoelectronic sequence. Checking the accuracy of calculations for other levels (including the highest levels) allows us to assert that position errors are limited to less than 1 eV.

Figure 1 shows the promising laser transitions in Ne-like Ar. The excitation energies of active levels as well as the energy of Ne-like argon created from Na-like ions and the ionization potential of Ne-like Ar are presented. The wavelength for each possible laser transition is supplied with the calculated radiative transition probability and the branch coefficient (the last one shows which part of the upper level population decays in a given low active level).

According to performed calculations, four lines in Ne-like Ar are

strongest for possible lasing:

$2p_{1/2}\ 3p_{3/2}$ [J=2] - $2p_{1/2}\ 3s_{1/2}$ [J=1], λ =697.6 Å,

$2p_{3/2}\ 3p_{3/2}$ [J=0] - $2p_{3/2}\ 3s_{1/2}$ [J=1], λ =430.7 Å,

$2p_{1/2}\ 3p_{1/2}$ [J=0] - $2p_{1/2}\ 3s_{1/2}$ [J=1], λ =712.5 Å,

$2p_{1/2}\ 3p_{1/2}$ [J=1] - $2p_{1/2}\ 3s_{1/2}$ [J=1], λ =727.5 Å.

Special attention should be paid to the level $2s2p^6 3s$ [J=0] which corresponds to the excitation of the 2s electron subshell. The energy of this level excitation in Ne-like Ar is comparatively high (330 eV); nevertheless, the electron collision rate for its population is high enough to provide an efficient inversion population relative to the low active level $2p_{3/2}3s_{1/2}$[J=1]. So the search for lasing at the transition

$2s_{1/2}\ 3s_{1/2}$ [J=0] - $2p_{3/2}\ 3s_{1/2}$ [J=1], λ =157.3 Å,

of Ne-like Ar will be of significant interest.

The numerical results of calculation for states $3p^6\ 3d^9$ 4s, 4p, 4d, 4f and $3p^5\ 3d^{10}$ 4s, 4p, 4d, 4f of Ni-like krypton are given in Table 2. For Ni-like ions levels $3d_{3/2}\ 4p_{1/2}$ [J=1], $3d_{3/2}\ 4p_{3/2}$ [J=1], and $3d_{3/2}\ 4p_{3/2}$ [J=1] can serve as low active levels.

Four laser transitions are possible here:

$3d_{5/2}\ 4d_{5/2}$ [J=0] - $3d_{3/2}\ 4p_{1/2}$ [J=1], λ =312.1 Å,

$3d_{3/2}\ 4d_{3/2}$ [J=0] - $3d_{3/2}\ 4p_{1/2}$ [J=1], λ =425.6 Å,

$3d_{3/2}\ 4d_{3/2}$ [J=1] - $3d_{3/2}\ 4p_{1/2}$ [J=1], λ =415.0 Å,

$3d_{3/2}\ 4d_{5/2}$ [J=2] - $3d_{3/2}\ 4p_{3/2}$ [J=1], λ =417.8 Å.

This approach gives us a quick method of evaluating laser possibilities for any ion. Nevertheless, it is necessary to look completely through the transition probability matrix to determine the second and third most important decay channels. Thus we are able to understand that in Kr IX the decay from the high active levels is almost equally distributed between three low active levels. The laser scheme for Kr IX is presented in Figure 2. The most favorable cases are for $3d_{3/2}\ 4d_{3/2}$ [J=0] and for $3d_{5/2}\ 4d_{5/2}$ [J=0] high active states. They have a relatively large branch coefficient for the transitions to low active level. In Figure 2 the very high active level $3p_{3/2}\ 4p_{3/2}$ [J=0] is also shown which corresponds to fast 3p subshell excitation.

At the same electron temperature, the collision excitation rate of

these levels is approximately the same as the excitation rate of both of the above-mentioned levels with J=0. However, there is no well-separated dominant channel for radiative transition into the fast releasing low active level.

The configuration 3p4p is buried into the dense spectrum of 3d5l and 3d6l configurations. A more reliable prediction for a laser scheme for Kr IX requires the inclusion of these configurations into the consideration. We have confirmed our results by taking into account the states of the 3d5l configuration.

In Table 3 we list calculated energy levels and radiative characteristics of Ni-like molybdenum. These data are interesting for two reasons. First, molybdenum could be a possible experimental material if we use a gaseous molybdenum compound (with low z elements) as a medium for a capillary discharge. Second, Ni-like laser scheme changes along the isoelectronic sequence are of appreciable interest. Our preliminary calculations of the Ni-like isoelectronic sequence spectroscopic properties have shown that intensity ratios of lasing transitions vary significantly with Z. This is caused by large differences in the radiative decay probability's dependence on Z. Branch coefficients may also vary significantly along Z. Consider the lowest active level in Ni-like ions $3d_{5/2}\ 4p_{3/2}$ [J=1] as an example. At low-Z value (Z < 50) it does not serve very effectively as a low active level for lasing because of the slow decay of this level into the ground state. However, at Z > 60 the decay probability of this level into the ground state becomes the largest of three low active levels. Thus, for heavy elements this level becomes the main lasing level of the three low active levels.

The laser scheme for Ni-like molybdenum is shown in Figure 3. The following three transitions are promising for lasing:

$3d_{5/2}\ 4d_{5/2}$ [J=0] - $3d_{3/2}\ 4p_{1/2}$ [J=1], λ =179.8 Å,

$3d_{3/2}\ 4d_{5/2}$ [J=2] - $3d_{3/2}\ 4p_{3/2}$ [J=1], λ =251.5 Å,

$3d_{3/2}\ 4d_{3/2}$ [J=1] - $3d_{3/2}\ 4p_{1/2}$ [J=1], λ =253.7 Å.

The first two should have approximately equal intensities, and the last one is less intensive. In Ni-like Mo two very high positioned levels $3p_{3/2}\ 4p_{3/2}$ [J=0] and $3p_{1/2}\ 4p_{1/2}$ [J=0] are also promising for lasing. According to our calculations they are well populated by electron collisions and have rather high branch coefficients of transitions to low active levels. Thus, the short-wavelength lines

$3p_{1/2}\ 4p_{1/2}$ [J=0] - $3d_{3/2}\ 4p_{1/2}$ [J=1], λ =68.0 Å,

$3p_{3/2}\ 4p_{3/2}$ [J=0] - $3d_{3/2}\ 4p_{1/2}$ [J=1], λ =73.5 Å,

should be investigated in more detail experimentally by

spectroscopic methods.

The level $3d_{3/2}$ $4d_{3/2}$ [J=1] is not included in this scheme because it has a small branch coefficient for transitions to low active levels.

According to our estimation, in the collisional exitation scheme with a long plasma life-time, the electron temperature which is sufficient for strong collisional exitation of upper active levels and lasing to occur is in the same range as the temperature to effectively ionize parent ions. For Ne-like Ar and Ni-like Kr we should be able to heat plasma to $T_e \approx 25$ eV to get lasing, and the Ni-like Mo scheme requires $T_e = 40$ eV. with λ = 179.8, 253.7 Å should take place with approximately equal intensities. The transition at λ =251.5 Å is of lesser intensity.

CONCLUSIONS

The present theory should be considered as a preliminary evaluation of plasma parameters required to obtain lasing at definite transitions of Ne-like and Ni-like ions of low charge multiplicity. Energetic characteristics of laser schemes given here demand a plasma electron temperature of 20-25 eV for laser action to occur at 4d-4p transitions in Ni-like krypton by a collisional pumping mechanism of active level populations. A plasma electron temperature of 25-30 eV is sufficient to produce lasing at 3p-3s transitions of Ne-like Argon.

Our study confirms that a Ni-like laser plasma consumes appreciably less input energy at shorter wavelengths than a Ne-like laser plasma. However, the Ni-like scheme demands a few times more electron density to achieve a sufficient gain coefficient. This is due to the larger number of levels in Ni-like ion as compared with the Ne-like ion. Also, the Ni-like scheme has three low active levels instead of two low active levels in the Ne-like scheme, so the branch coefficients for radiative transition probabilities from high active levels to low ones in the Ni-like scheme are significantly less than in the Ne-like case.

We believe that for both elements the plasma conditions for producing laser radiation can be achieved using a capillary discharge design. The most surprising result of this work is the prediction that there is a possibility of observing lasing from 3p-3d (vacancy transitions) with wavelengths of 90-100 Å at electron temperatures of 25-30 eV with a collision pumping mechanism of a population of 3p4p highly excited states. Calculations of electron collisional rates of excitation of heavy Ni-like ions with $60 < Z < 92$ were done, which showed that the collisional excitation rate of highly excited 3p4p [J=0] states is of the same order as the excitation rate of 3d4d [J=0] states under the same electron temperatures [27]. That encourages us to suppose the validity of this statement for lighter Ni like ions.

A more exact calculations that investigates the possibility of generating laser radiation at the 3p-3d transitions of Ni-like Kr are being performed now. It will draw on the foundation of these calculations but will include the dense spectrum of 3d5l configurations.

EXPERIMENT

We have begun to design and to assemble the capillary discharge x-ray laser setup based on our preliminary estimations of plasma parameters required for ASE to occur. The energy storage compact low-inductance capacitor C=0.2 uF with U_{max}=100 kV and L_{tot}=20 nH was choosen to drive the discharge current up to 50 kA. This capillary discharge is a prototype for a future Phase II experimental setup. The current capillary discharge design allows us to vary the capillary diameter in the 0.1-3.0 mm range and the length in the 20 - 120 mm range. In our final report we will describe in more detail our design along with the results of MHD simulation of the capillary plasma.

Table 1.
Energy levels and radiative characteristics of Ne-like Argon.
Ar IX (Z=18)

1	2	3	4	5	6	7	8	9	10	11
#	Level	J	Eexper (sm-1)	Eth (sm-1)	Probab n-0 (sec-1)	Life time (psec)	i	Branch coeff. n - i	Wave length (A)	Wavel exper [28]
0	2s2 2p6	0	0	0						
1	2p3/2 3s1/2	2	2026542	2026504	.13+04					
2	2p3/2 3s1/2	1	2033120	2033273	.50+11					
3	2p1/2 3s1/2	0	2044670	2044390	.0					
4	2p1/2 3s1/2	1	2051880	2052270	.14+12					
5	2p3/2 3p3/2	1	2149320	2149800	.60+05	441	1	.42	811.1	814.5
6	2p3/2 3p3/2	3	2169894	2169600	.45+00	460	1	1.0	698.8	697.6
7	2p3/2 3p1/2	2	2170923	2170620	.83+07	492	1	.46	693.8	692.6
8	2p3/2 3p1/2	1	2176716	2176320	.83+04	481	1	.42	667.5	665.9
9	2p3/2 3p3/2	2	2182224	2181790	.16+08	456	1	.50	644.0	642.3
10	2p1/2 3p1/2	1	2189330	2188900	.13+05	490	4	.45	731.9	727.5+
11	2p1/2 3p1/2	0	2192240	2191620	.0	480	4	.55	717.6	712.5+
12	2p1/2 3p3/2	2	2195230	2194790	.19+08	458	4	.79	701.7	697.6+
13	2p1/2 3p3/2	1	2196230	2195540	.76+04	462	3	.55	661.6	659.8
14	2p3/2 3p3/2	0	2265320	2271360	.0	470	2	.57	420.0	430.7+
15	2p3/2 3d3/2	0	2349300	2348603	.0	152	8	.43	580.5	579.4
16	2p3/2 3d3/2	1	2351420	2350700	.60+10	81	8	.14	573.5	572.4
17	2p3/2 3d5/2	2	2355570	2354950	.34+05	158	9	.24	577.5	576.9
18	2p3/2 3d5/2	4	2358730	2358660	.87-04	159	6	1.0	529.1	529.6
19	2p3/2 3d3/2	3	2361760	2361960	.11+04	154	7	.73	522.7	524.0
20	2p3/2 3d3/2	2	2366960	2366990	.24+04	154	7	.27	509.3	510.1
21	2p3/2 3d5/2	3	2370655	2371530	.33+04	159	9	.76	527.0	530.7
22	2p3/2 3d5/2	1	2381120	2381490	.14+12	7	11	.01	526.7	529.4
23	2p1/2 3d3/2	2	2382450	2382700	.45+04	154	10	.51	516.0	517.8
24	2p1/2 3d5/2	3	2384880	2385380	.25+04	159	12	.84	524.7	527.3
25	2p1/2 3d5/2	2	2385380	2385430	.77+02	159	13	.56	526.6	528.7
26	2p1/2 3d3/2	1	2411310	2418700	.32+13	0.3	11	.001	439.8	456.5
27	2s1/2 3s1/2	1		2639720	.18+04	51	1	.59	163.1	
28	2s1/2 3s1/2	0		2668780	.0	51	2	.64	157.3+	
29	2s1/2 3p1/2	0		2780200	.0	46	10	.32	169.1	
30	2s1/2 3p1/2	1		2781050	.82+10	34	7	.28	163.8	
31	2s1/2 3p3/2	2		2783390	.76+04	46	6	.44	162.9	
32	2s1/2 3p3/2	1	2791700	2792670	.44+12	2	9	.01	163.7	164.1
33	2s1/2 3d3/2	1		2967370	.60+02	38	23	.18	171.0	
34	2s1/2 3d3/2	2		2967470	.15+05	38	19	.21	165.1	
35	2s1/2 3d5/2	3		2967600	.84+01	39	18	.34	164.2	
36	2s1/2 3d5/2	2		2984800	.36+09	38	19	.14	160.5	

+) possible laser transitions

Table 2.
Energy levels and radiative characteristics of Ni-like Krypton.
Kr IX (Z=36)

1	2	3	4	5	6	7	8	9	10	11
#	Level	J	Eexp (sm-1)	Eth (sm-1)	Probab n-0 (sec-1)	Life time (psec)	i	Branch coeff. n - i	Wave length (A)	Wave exp (A)
0	3p5 3d10	0	0	0						
1	3d5/2 4s1/2	3	690437	690336	.86-05					
2	3d5/2 4s1/2	2	693422	693590	.12+05					
3	3d3/2 4s1/2	1	700749	700710	.76-02					
4	3d3/2 4s1/2	2	704584	705230	.40+05					
5	3d5/2 4p1/2	2	838759	838870	.78+01	247	1	.67	673.2	674.2
6	3d5/2 4p1/2	3	844265	844410	.76+00	258	2	.47	663.0	662.9
7	3d5/2 4p3/2	1	849546	849700	.16+09	212	2	.43	640.6	640.5*
8	3d3/2 4p1/2	2	852008	851850	.17+00	252	3	.42	661.6	661.1
9	3d5/2 4p3/2	4	852311	852240	.12-08	206	1	1.0	617.6	617.8
10	3d3/2 4p3/2	0	856140	856290	.00	206	3	1.0	642.8	643.5
11	3d5/2 4p3/2	2	860273	860770	.65+01	219	2	.54	598.2	599.3
12	3d5/2 4p3/2	3	861782	862190	.12+01	206	1	.51	581.9	583.6
13	3d3/2 4p1/2	1	863998	865930	.30+11	30	4	.06	622.3	627.3*
14	3d3/2 4p3/2	3	866442	866630	.11+01	207	4	.80	619.6	617.8
15	3d3/2 4p3/2	1	869958	870850	.18+10	44	3	.12	587.8	591.0*
16	3d3/2 4p3/2	2	871943	872220	.60+00	208	3	.49	583.0	584.1
17	3d5/2 4d3/2	1	1081246	1081290	.47+06	42	5	.38	412.5	412.4
18	3d5/2 4d5/2	5	1093152	1091740	.00	44	9	1.0	417.6	415.2
19	3d5/2 4d3/2	4	1093033	1091987	.17-03	41	6	.77	403.9	402.0
20	3d5/2 4d3/2	2	1093778	1092930	.19+04	41	5	.39	393.6	392.1
21	3d5/2 4d5/2	1	1093894	1092970	.42+05	42	5	.33	393.5	392.0
22	3d5/2 4d3/2	3	1096690	1095907	.16-02	42	6	.25	397.6	396.1
23	3d5/2 4d5/2	3	1098421	1097390	.88-03	42	8	.22	407.3	405.8
24	3d3/2 4d3/2	0	1098968	1098060	.00	41	13	.47	430.8	425.6+
25	3d5/2 4d5/2	2	1099903	1099140	.60+06	43	11	.25	419.5	417.3
26	3d5/2 4d5/2	4	1100439	1099440	.18-03	44	12	.60	421.5	419.0
27	3d3/2 4d5/2	1	1101083	1100250	.13+06	42	10	.29	409.9	408.2
28	3d3/2 4d3/2	3	1104304	1103420	.39-03	41	8	.48	397.5	396.3
29	3d3/2 4d3/2	1	1105020	1104320	.73+05	41	13	.35	419.5	414.9+
30	3d3/2 4d5/2	4	1106607	1105570	.19-03	44	14	.78	418.5	416.4
31	3d3/2 4d5/2	2	1109305	1108510	.59+06	43	15	.35	420.8	417.8+
32	3d3/2 4d5/2	3	1111320	1110470	.15-04	43	16	.67	419.7	417.8
33	3d3/2 4d3/2	2	1111363	1110860	.14+07	40	8	.33	386.1	385.6
34	3d5/2 4d5/2	0	1184400	1185970	.00	42	13	.43	312.5	312.1+

* measured wavelengthes [30]; all other figures in this coulomn and in 4th coulomn are compilation [31].

+ possible laser transitions

Table 2. (cont.)

1	2	3	4	5	6	7	8	9	10	11
#	Level	J	Eexp (sm-1)	Eth (sm-1)	Probab n-0 (sec-1)	Life time (psec)	i	Branch coeff. n - i	Wave length (A)	Wave exp (A)
35	3d5/2 4f5/2	0		1299930	.00	37	17	.50	457.4	
36	3d5/2 4f5/2	1		1301470	.63+09	36	17	.28	454.2	
37	3d5/2 4f7/2	2		1304450	.11+04	37	20	.21	472.8	
38	3d5/2 4f5/2	5		1305370	.71-07	37	19	.87	468.6	
39	3d5/2 4f7/2	6		1306300	.00	37	18	1.0	466.0	
40	3d5/2 4f5/2	2		1308180	.80+03	37	20	.28	464.6	
41	3d5/2 4f5/2	3		1308530	.75-00	37	20	.29	463.8	
42	3d5/2 4f5/2	4		1309360	.11-07	37	23	.33	468.5	
43	3d5/2 4f7/2	4		1310800	.68-06	37	23	.28	468.6	
44	3d5/2 4f7/2	5		1311540	.45-07	37	26	.70	471.5	
45	3d5/2 4f7/2	3		1311830	.13+03	37	25	.27	470.1	
46	3d5/2 4f7/2	1		1311900	.27+11	19	34	.09	794.1	
47	3d3/2 4f7/2	2		1316110	.14+02	37	27	.35	463.3	
48	3d3/2 4f5/2	4		1316450	.54-07	37	28	.55	469.4	
49	3d3/2 4f5/2	2		1318700	.23+03	37	29	.36	466.5	
50	3d3/2 4f7/2	5		1318770	.66-07	37	30	.80	469.0	
51	3d3/2 4f7/2	3		1321120	.15+02	37	31	.55	470.3	
52	3d3/2 4f5/2	3		1321720	.16+03	37	33	.56	474.2	
53	3d3/2 4f7/2	4		1322510	.46-09	37	32	.79	471.5	
54	3d3/2 4f5/2	1		1336970	.95+12	1	24	.006	418.6	
55	3p3/2 4s1/2	2		1642750	.59+03	4	1	.84	104.9	
56	3p3/2 4s1/2	1		1649025	.93+11	3	2	.58	104.6	
57	3p1/2 4s1/2	0		1706230	.00	3	3	1.0	99.4	
58	3p1/2 4s1/2	1		1709940	.61+11	3	4	.60	99.5	
59	3p3/2 4p1/2	1		1789880	.42+6	4	5	.52	105.0	
60	3p3/2 4p1/2	2		1797430	.10+08	4	6	.78	104.9	
61	3p3/2 4p3/2	3		1805200	.16+00	4	9	.76	104.9	
62	3p3/2 4p3/2	1		1809030	.31+06	4	11	.36	105.4	
63	3p3/2 4p3/2	2		1814290	.86+07	4	12	.60	105.0	
64	3p3/2 4p3/2	0		1832990	.00	4	7	.39	101.6	
65	3p1/2 4p1/2	1		1859680	.47+05	3	8	.67	99.2	
66	3p1/2 4p3/2	1		1872290	.70+02	3	16	.37	100.0	
67	3p1/2 4p3/2	2		1872890	.11+08	3	14	.61	99.3	

Table 3.
Energy levels and radiative characteristics of Ni-like Molybdenium.
Mo XV (Z=42)

1	2	3	4	5	6	7	8	9	10	11
#	Level	J	Eexp (sm-1)	Eth (sm-1)	Probab n-0 (sec-1)	Life time (psec)	i	Branch coeff. n - i	Wave length (A)	Wavel exp (A)
0	3p53d10	0	0	0						
1	3d5/2 4s1/2	3	1694913	1694588	.89-01					
2	3d5/2 4s1/2	2	1699860	1699821	.39+07					
3	3d3/2 4s1/2	1	1721768	1721310	.93-01					
4	3d3/2 4s1/2	2	1726414	1726530	.59+07					
5	3d5/2 4p1/2	2	1932855	1931860	.15+04	112	1	.70	421.5	420.3
6	3d5/2 4p1/2	3	1939450	1939190	.43+03	125	2	.52	417.8	417.3
7	3d3/2 4p1/2	2	1962158	1961510	.46+02	119	3	.43	416.3	416.0
8	3d5/2 4p3/2	1	1963618	1962556	.10+09	91	2	.45	380.6	379.1
9	3d5/2 4p3/2	4	1968194	1967600	.20-04	82	1	1.0	366.3	365.9
10	3d5/2 4p3/2	2	1978021	1978100	.17+04	86	2	.65	359.3	359.5
11	3d5/2 4p3/2	3	1982272	1982900	.40+03	82	1	.55	346.8	348.0
12	3d3/2 4p3/2	0	1982912	1983570	.00+00	77	3	1.0	381.3	382.9
13	3d3/2 4p1/2	1	1984954	1983570	.30+12	3	2	.02	352.4	350.8
14	3d3/2 4p3/2	3	1999877	1999600	.62+03	82	4	.95	366.2	365.7
15	3d3/2 4p3/2	1	2003415	2003530	.75+11	11	3	.10	354.3	355.0
16	3d3/2 4p3/2	2	2008192	2008170	.42+02	82	3	.49	348.6	349.1
17	3d5/2 4d3/2	1		2342010	.13+07	18	5	.50	243.8	
18	3d5/2 4d3/2	4		2361940	.13+00	17	6	.82	236.5	
19	3d5/2 4d3/2	2		2363500	.11+06	17	5	.50	231.7	
20	3d5/2 4d5/2	5		2364540	.72-08	20	9	1.0	251.9	
21	3d5/2 4d5/2	1		2364740	.12+07	19	5	.32	231.0	
22	3d5/2 4d3/2	3		2369420	.52+00	18	6	.36	232.4	
23	3d5/2 4d5/2	3		2374400	.74+00	19	11	.30	255.4	
24	3d5/2 4d5/2	2		2377240	.25+08	19	10	.34	250.5	
25	3d3/2 4d3/2	0		2377800	.00	18	13	.45	253.7+	
26	3d5/2 4d5/2	4		2378590	.83-01	20	11	.70	252.7	
27	3d3/2 4d5/2	1		2384670	.44+06	18	12	.22	249.3	
28	3d3/2 4d3/2	3		2389110	.11-00	17	7	.66	233.9	
29	3d3/2 4d3/2	1		2392260	.12+06	18	12	.25	244.7	
30	3d3/2 4d5/2	4		2396470	.14-00	20	14	.93	252.0	
31	3d3/2 4d5/2	2		2401170	.13+08	20	15	.46	251.5+	
32	3d3/2 4d3/2	2		2403050	.40+08	17	7	.36	226.5	
33	3d3/2 4d5/2	3		2405540	.48-03	20	16	.72	251.7	
34	3d5/2 4d5/2	0		2539640	.00	17	13	.45	179.8+	

Table 3 (cont.)

1	2	3	4	5	6	7	8	9	10	11
#	Level	J	Eexp (sm-1)	Eth (sm-1)	Probab n-0 (sec-1)	Life time (psec)	i	Branch coeff. n - i	Wave length (A)	Wavel exp. (A)
35	3d5/2 4f5/2	0		2756650	.00	15	17	.58	241.2	
36	3d5/2 4f5/2	1	2749060	2759538	.17+11	12	17	.26	239.5	
37	3d5/2 4f7/2	2		2764348	.13+06	15	21	.25	250.2	
38	3d5/2 4f7/2	6		2767980	.00	15	20	1.0	247.9	
39	3d5/2 4f5/2	5		2770160	.29-04	15	18	.88	245.0	
40	3d5/2 4f5/2	2		2774590	.38+05	15	19	.36	243.3	
41	3d5/2 4f7/2	3		2775130	.31+03	15	24	.26	251.3	
42	3d5/2 4f7/2	4		2777590	.48-03	15	23	.45	248.0	
43	3d5/2 4f5/2	4		2779190	.55-04	15	22	.43	244.0	
44	3d5/2 4f7/2	5		2780150	.15-04	15	26	.77	249.0	
45	3d5/2 4f5/2	3		2782160	.10+05	15	24	.26	247.0	
46	3d5/2 4f7/2	1	2773160	2784410	.27+12	3	34	.03	408.5	
47	3d3/2 4f7/2	2		2793240	.32+02	15	29	.34	249.4	
48	3d3/2 4f5/2	4		2797720	.24-04	15	28	.71	244.7	
49	3d3/2 4f7/2	5		2799490	.30-04	15	30	.90	248.1	
50	3d3/2 4f5/2	2		2802150	.21+05	15	29	.30	244.0	
51	3d3/2 4f7/2	3		2804670	.44+04	15	31	.70	247.8	
52	3d3/2 4f7/2	4		2807820	.46-05	15	33	.80	248.6	
53	3d3/2 4f5/2	3		2809750	.92+04	15	32	.69	246.9	
54	3d3/2 4f5/2	1	2827410	2849950	.74+13	.1	25	.002	211.8	
55	3p3/2 4s1/2	2		3018660	.10+05	3	1	.85	75.5	
56	3p3/2 4s1/2	1		3028200	.28+12	2	2	.50	75.3	
57	3p1/2 4s1/2	0		3162950	.00	2	3	1.0	69.4	
58	3p1/2 4s1/2	1		3168350	.17+12	1	4	.60	69.4	
59	3p3/2 4p1/2	1		3255860	.24+06	3	5	.71	75.5	
60	3p3/2 4p1/2	2		3263650	.98+08	3	6	.81	75.5	
61	3p3/2 4p3/2	3		3292160	.77+01	3	9	.75	75.5	
62	3p3/2 4p3/2	1		3295580	.32+05	3	10	.45	75.9	
63	3p3/2 4p3/2	2		3306240	.88+08	3	11	.64	75.6	
64	3p3/2 4p3/2	0		3343750	.00	2	13	.42	73.5+	
65	3p1/2 4p1/2	1		3405710	.78+04	2	7	.72	69.2	
66	3p1/2 4p3/2	1		3441400	.10+06	2	16	.39	69.8	
67	3p1/2 4p3/2	2		3442940	.10+09	2	14	.67	69.3	
68	3p1/2 4p1/2	0		3453190	.00	2	13	.50	68.0+	

+ possible laser transitions

Table 3 (cont.)

1	2	3	4	5	6	7	8	9	10	11
#	Level	J	Eexp (sm-1)	Eth (sm-1)	Probab n-0 (sec-1)	Life time (psec)	i	Branch coeff. n - i	Wave length (A)	Wavel exp. (A)
69	3p3/2 4d3/2	0		3675950	.00	3	17	.50	75.0	
70	3p3/2 4d3/2	1		3680980	.46+11	2	19	.30	75.9	
71	3p3/2 4d3/2	3		3686980	.44+05	2	18	.64	75.5	
72	3p3/2 4d5/2	4		3689840	.40-02	2	20	.65	75.5	
73	3p3/2 4d5/2	2		3690750	.45+05	2	22	.24	75.7	
74	3p3/2 4d3/2	2		3697300	.38+05	2	22	.26	75.3	
75	3p3/2 4d5/2	1		3700310	.14+13	.5	21	.04	74.9	
76	3p3/2 4d5/2	3		3702110	.22+05	2	26	.50	75.6	
77	3p1/2 4d3/2	2		3832350	.12+03	2	28	.53	69.3	
78	3p1/2 4d5/2	2		3838810	.99+04	2	31	.31	69.6	
79	3p1/2 4d3/2	1		3838930	.71+12	1	32	.15	69.6	
80	3p1/2 4d5/2	3		3839900	.37+05	2	30	.55	69.3	
81	3p3/2 4f5/2	1		4082851	.91+03	2	36	.27	75.6	
82	3p3/2 4f5/2	2		4087500	.17+09	2	40	.16	76.2	
83	3p3/2 4f5/2	4		4088470	.24+02	2	39	.58	75.9	
84	3p3/2 4f7/2	5		4088910	.24-05	2	38	.61	75.7	
85	3p3/2 4f7/2	3		4094400	.12+03	2	42	.24	75.9	
86	3p3/2 4f5/2	3		4100530	.13+02	2	43	.36	75.8	
87	3p3/2 4f7/2	4		4100560	.55+01	2	44	.41	75.7	
88	3p3/2 4f7/2	2		4106550	.16+10	2	37	.15	74.5	
89	3p1/2 4f7/2	4		4237980	.16+02	2	49	.51	69.5	
90	3p1/2 4f5/2	3		4238400	.52+01	2	48	.50	69.4	
91	3p1/2 4f7/2	3		4238840	.34+02	2	51	.31	69.7	

FIGURE CAPTIONS.

1. A simplified energy level diagram for Ne-like Ar showing possible laser transitions.

2. A simplified energy level diagram for Ni-like Kr showing possible laser transitions.

3. A simplified energy level diagram for Ni-like Mo showing possible laser transitions.

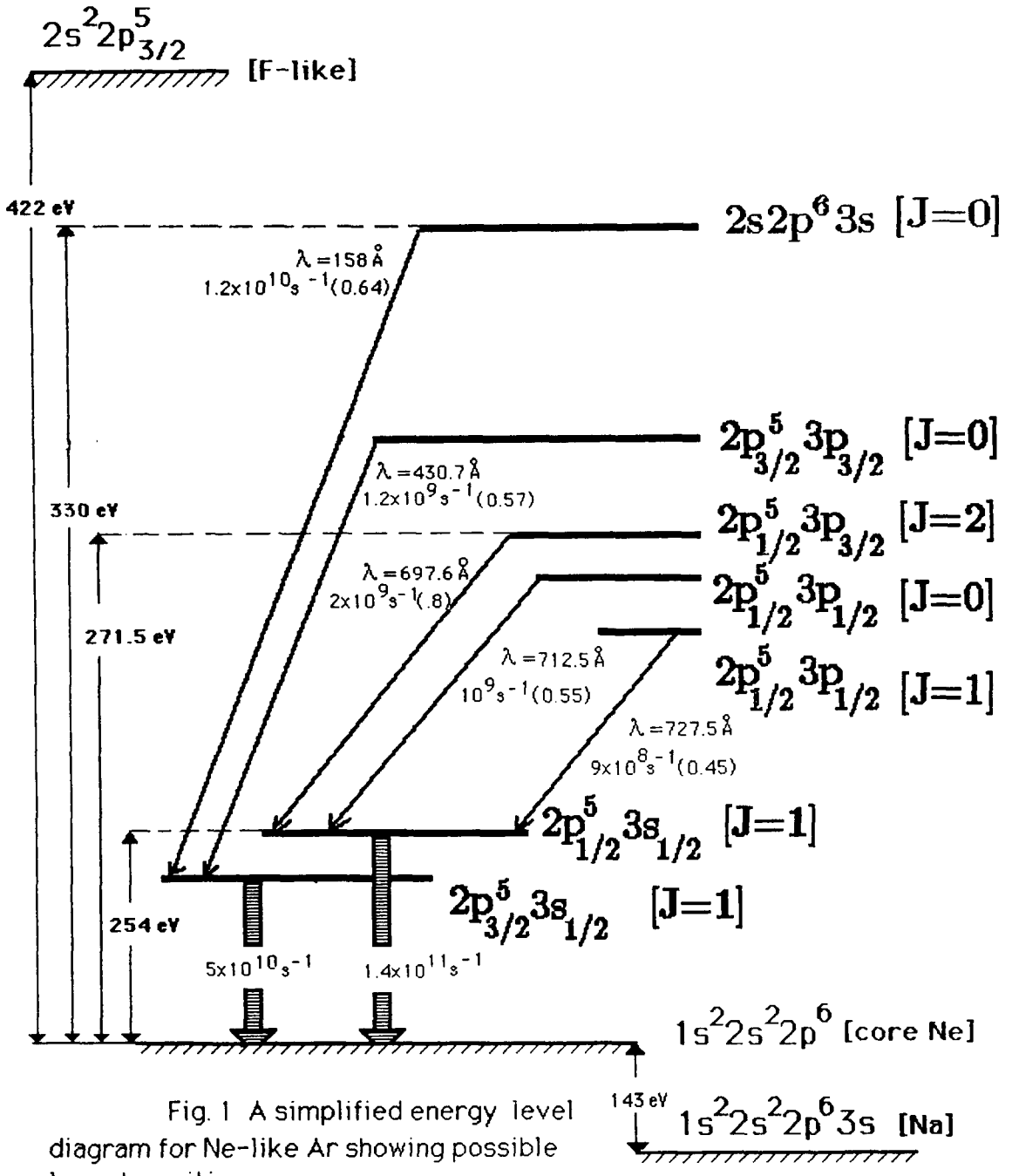

Fig. 1 A simplified energy level diagram for Ne-like Ar showing possible laser transitions.

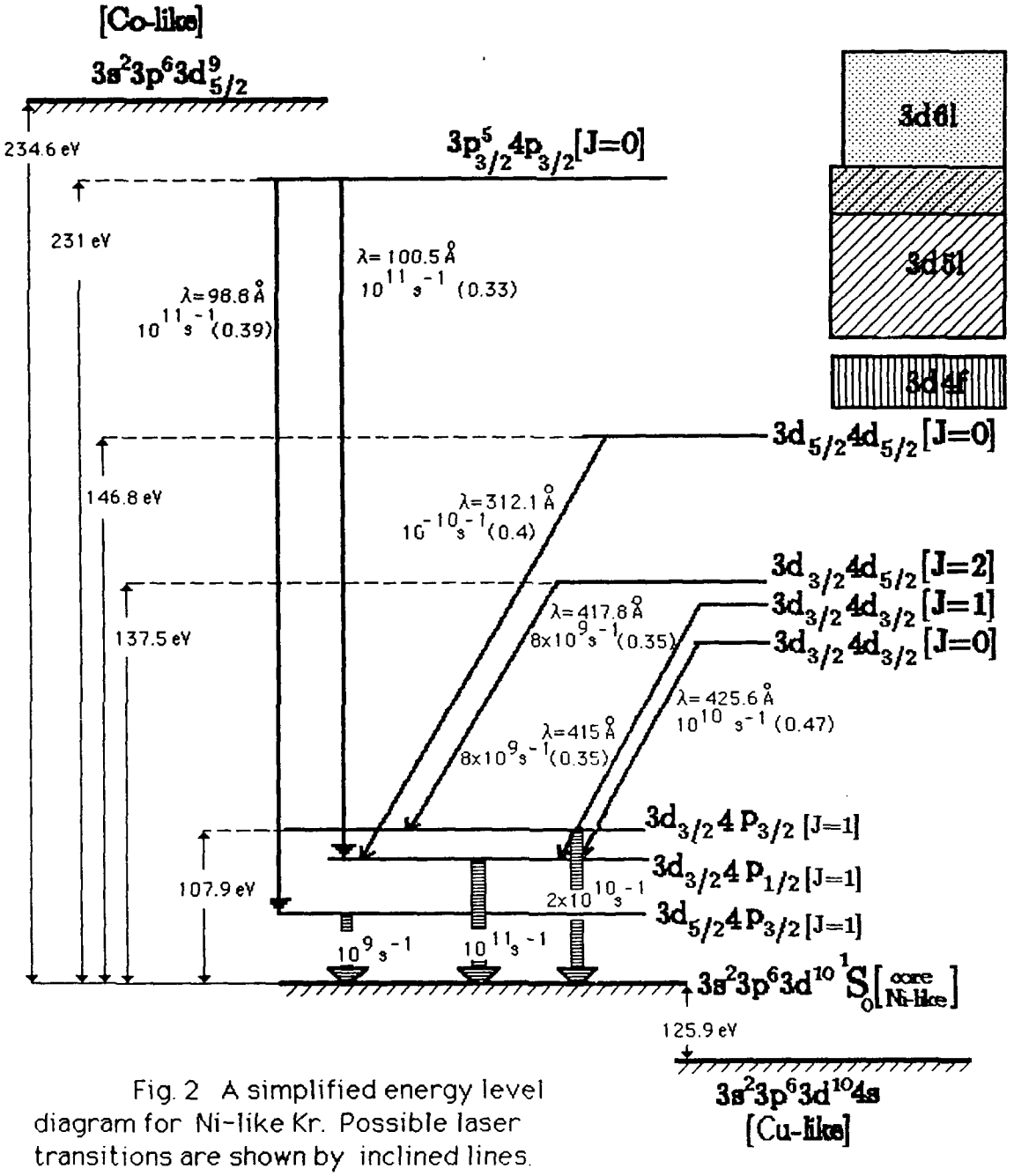

Fig. 2 A simplified energy level diagram for Ni-like Kr. Possible laser transitions are shown by inclined lines.

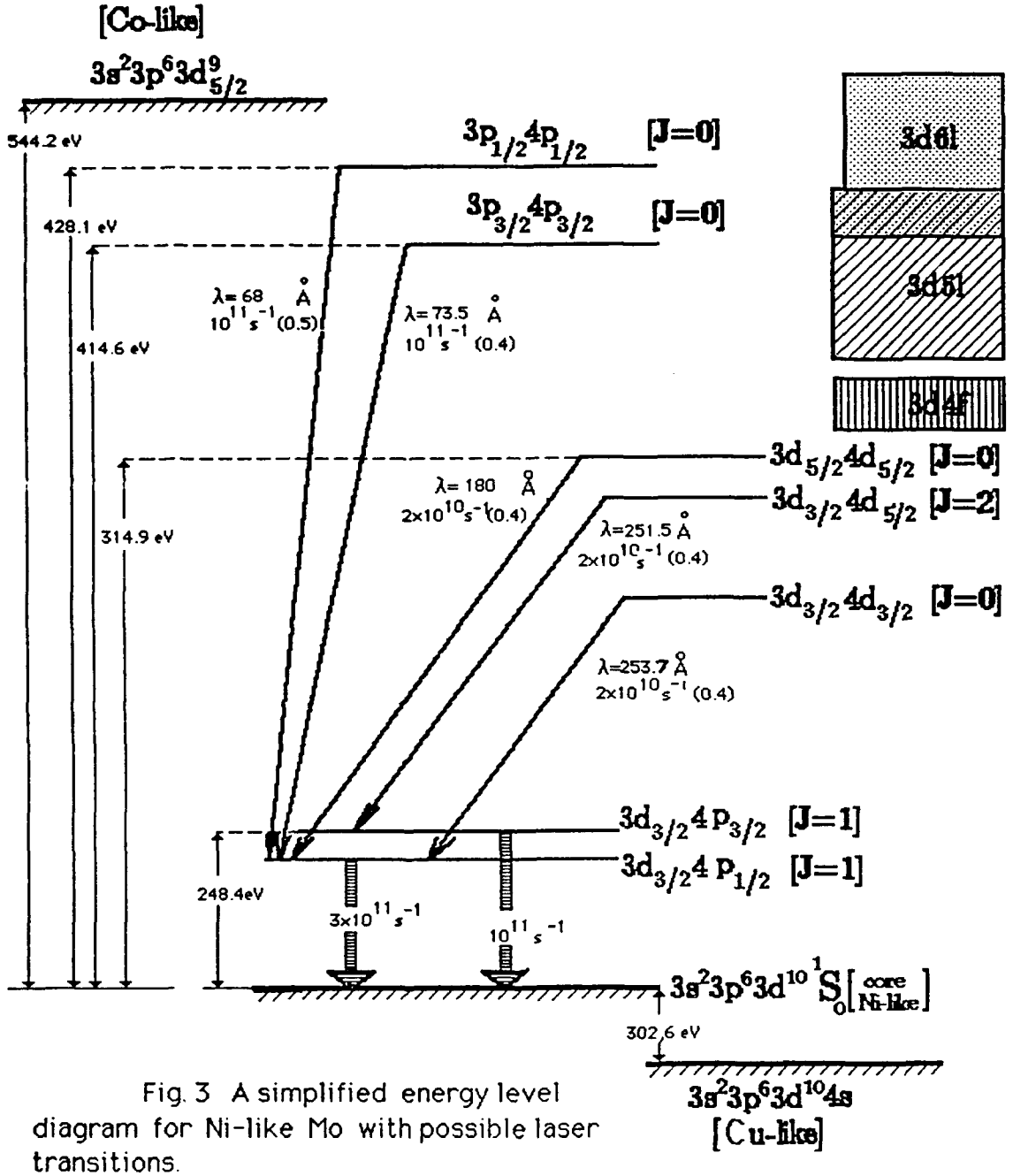

Fig. 3 A simplified energy level diagram for Ni-like Mo with possible laser transitions.

REFERENCES:

1. A. G. Molchanov, Sov. Phys. Uspekhi, 15, 124 (1972).

2. R. C. Elton, Appl. Optics, 14, 97 (1975).

3. D. L. Matthews et al., Phys. Rev. Lett., 54, 110 (1985).

4. M. D. Rosen, P. L. Hagelstein, D. L. Matthews et al., Phys. Rev. Lett., 54, 106 (1985).

5. T. Boehly et. al, Phys. Rev. A42, 3626 (1990).

6. T. N. Lee, E. A. McLean, and R. C. Elton, Phys. Rev. Lett, 59, 1185 (1987).

7. D. Naccache et. al, Phys. Rev. A42, 3027 (1990).

8. S. Wang et al., Chinese Phys. Lett., 8, 618 (1991).

9. G. D. Enright et. al, J. Opt. Soc. Am., 8, 2047 (1991).

10. J. W. Thornhill, J. Davis, J. P. Apruzese, and R. Clark, Appl. Optics, 31, 24, 4940 (1992).

11. B. J. MacGowan et al., Phys. Rev. Lett., 59, 2157 (1987).

12. B. J. MacGowan et al., J. Opt. Soc. Am. B, 5, 1858 (1988).

13. E. P. Ivanova and A. V. Gulov, At. Data Nucl. Data Tables, 49, 1 (1991).

14. B. C. Fawcett, and R. V. Haues, Phys. Scripta, 36, 80, (1987).

15. E. V. Aglitsky, E. P. Ivanova, A. M. Panin, U. I. Safronova, S. A. Ulitin, L. A. Vainstein, and J. F. Wyart, Phys. Scripta, 38, 136 (1988).

16. P. L. Hagelstein and R. K. Jung, At. Data Nucl. Data Tables, 37, 121 (1987).

17. E. V. Aglitsky, P. S. Antsiferov, A. M. Panin and S. A. Ulitin, Sov. J. Optics & Spectroscopy, 60, 1, 197 (1986).

18. A. N. Ryabtsev and S. S. Churilov, Spectroscopy of multicharged ions in hot plasma (Russia), Moscow, Nauka (1991).

19. E. P. Ivanova and A. L. Gogava, Sov.J. Opt. Spectrosc. 59, 6 (1985).

20. T. Brage and U. Litzen, Phys. Scripta, 35, 62 (1987).

21. S. S. Churilov, A. N. Ryabtsev and J. F. Wyart, Phys. Scripta, 38, 326 (1988).

22. J. Nilsen, Phys. Rev. Lett., 66, 305 (1991).

23. E.P.Ivanova and A. V. Gulov, Phys. Lett.A, 140, 39 (1989)

24. L. N. Ivanov and M. N. Driker, Sov. J. Opt. Spectros., 49, 209 (1980).

25. V. V. Tolmachev, Adv. Chem. Phys., 14, 421, 471 (1969).

26. M. Gell-Mann and F. Low, Phys. Rev., 84, 350 (1951).

27. E. P. Ivanova, L. N. Ivanov, A. V. Glushkov, and A. E. Kramida, Phys. Scripta, 32, 513 (1985).

28. H. L. Zhang, D. H. Sampson, R. E. Clark, and J. B. Mann, At. Data Nucl. Data Tables, 37, 17 (1987).

29. A. E. Kramida, The identification of 3s-3p, 3p-3d transitions of Ne-like ions S VII, Cl VIII, Ar IX and K X, PhD Thesis.

30. J. Reader, A. N. Ryabtsev, A. A. Ramonas, J. Opt. Soc. Am. B.,2, 3, 417, (1985).

31. J. Sugar, A. Musgrove, J. Phys. Chem. Data, 20, 5, 859, (1991).